

1 **Gas Reservoir Detection Using Mixed Components Short Time Fourier**
2 **Transform (MC-STFT) as a new attribute**

3
4

5 **Gas Reservoir Detection Using Mixed Components Short Time Fourier**
6 **Transform (MC-STFT) as a new attribute**

7

8 **Ali Jalali¹, Majid Bagheri^{2*}, Mostafa Abbasi³**

9 1- PhD student, Institutes of Geophysics, University of Tehran, Tehran, Iran

10 2-Associate professor, Institutes of Geophysics, University of Tehran, Tehran, Iran

11 3-National Iranian oil company (NIOC), Tehran, Iran

12 * Corresponding author

13 Email: majidbagheri@ut.ac.ir

14 ORCID: 0000-0003-2059-0194

15

16

17 **Abstract**

18 Identification of gas reservoirs as a main natural resource due to its economic importance has
19 always been one of the most important issues in research studies in the oil and gas field. Accurate
20 localization of a gas reservoir through seismic data has been broadly studied. The final destination
21 of all seismic attributes is to distinguish a specific feature. Accordingly, many seismic attributes
22 have been developed among which short time Fourier transform (STFT)-based methods play an
23 important role. The location of gas reservoirs can be detected taking advantage of its particular
24 criteria in seismic data. Generally seismic signals are nonstationary as their frequency responses
25 vary with time. So we propose an attribute which utilizes mixed components of STFT (MC-STFT).
26 The novelty about this method is that without altering STFT method or adding any complexity,
27 MC-STFT is able to detect gas reservoirs at high resolution. [Simplicity and time efficiency can](#)
28 [make a method superior. In fact, this method takes advantage of extracting three frequency](#)

29 components obtained by STFT. In the next step, we can do the second iteration of the procedure,
30 this will represent the degree of sharpness of reduction in amplitude and again do the same jobs as
31 before and it leads to this, make it more specific. We apply this method on three data sets, first,
32 Marmousi model and then two other real seismic zero-offset sections. To evaluate the proposed
33 method compared with the Synchrosqueezing STFT (SSTFT). The results confirm good
34 performance of MC-STFT in high resolution gas reservoir detection.

35

36 **Keywords:** Gas reservoir, STFT, Seismic data, Attributes, Localization

37

38 **1. Introduction**

39 The location of gas reservoirs can be detected taking advantage of its particular criteria in seismic
40 data. Generally seismic signals are nonstationary as their frequency responses vary with time.
41 There are some techniques called Time-Frequency Decomposition (TFD) which map a 1D signal
42 into a 2D plane of time and frequency. In this way the frequency content of the signal with respect
43 to time can be revealed. So TFD methods used as spectral decomposition in both seismic
44 processing and interpretation (Reine et al., 2009; Chen et al., 2014). For example, Partyka et al.,
45 (1999) adopted the windowed discrete Fourier transform (DFT) for reservoir characterization. To
46 detect low frequency shadows beneath hydrocarbon reservoirs, Castagna et al., (2003) applied the
47 matching-pursuit decomposition. Sinha et al., (2005) proposed a novel method of taking a Fourier
48 transform of the inverse continuous wavelet transform (CWT) as a time-frequency map to identify
49 subtle stratigraphic features (Zhang et al., 2019). Wu and Zhou (2018) developed
50 synchrosqueezing wavelet transform (SWT) to reallocate the wavelet transform values to different
51 points and produce a sharp spectral decomposition for the input signal (Mateo et al., 2020). Li and
52 Zheng (2008) took advantage of the smoothed pseudo-Wigner-Ville distribution (SPWVD) for
53 carbonate reservoir characterization. Zhang and Lu (2010) applied the deconvolutive short-time
54 Fourier transform (DSTFT) method, which improves the time and frequency resolution of the
55 STFT spectrogram by 2D deconvolution on seismic spectral decomposition. Liu et al., (2011)
56 proposed a spectral decomposition method in which time-varying Fourier coefficients are used to
57 define a time-frequency map (Zhuang et al., 2020).

58 Spectral decomposition has been applied in exploration fields such as hydrocarbon detection,
 59 seismic attenuation analysis, channel identification, and thin-layer thickness estimation (Quan &
 60 Harris 1997, Gao et al. 1999, Liu & Marfurt 2007, Zhou et al. 2019, Odegard et al. 1997).
 61 Conventional spectral decompositions have some restrictions such as Heisenberg uncertainty
 62 principle and cross-terms which limit their applications in signal analysis. In an effort to overcome
 63 some of the limitations, use has been made of the STFT (Siddique et al., 2023; Yang et al., 2019).
 64 Recently, valuable efforts are done to cover these limitations, Barabadi et al., (2024) used
 65 synchroextracting transform for AVO analysis in time frequency and Shirazi et al., (2023)
 66 employed Multi-synchrosqueezing transform to detect shallows gas.

67 In this article we propose a novel seismic attribute to detect gas reservoirs which is based on STFT
 68 (Cohen, 1989). The superiority of this method relies not only on its simplicity (which doesn't add
 69 any mathematical burden to STFT method) but also on the high resolution characterization it
 70 provides. This method takes advantage of seismic low frequency shadows as a gas reservoir
 71 indicator. The novelty behind this algorithm is in seismic signal transformation from time domain
 72 to time-frequency domain using STFT and then extraction of three frequency sections of each
 73 signal. This approach converts seismic zero-offset section into a 2D image of gas reservoir.

74 We assess the performance of the proposed algorithm against three models including Marmousi
 75 model and other two real data. The results show that the first iteration of this algorithm can locate
 76 gas reservoirs at high resolution which can also be much more accurate by applying the second
 77 iteration in comparison to the method SSTFT.

78

79 2. Theory

80 2.1. Short Time Fourier Transform (STFT)

81 This section first deals with STFT formulation used in this study and then STFT-proceeding
 82 algorithm to obtain the final gas reservoir image.

83 The discrete time STFT method is formulated as

$$X_{STFT}[m, \omega] = \sum_{n=-\infty}^{\infty} x[n] w[n - m] e^{-i\omega n} \quad (1)$$

84

$$w(m) = ae^{-\frac{(m-b)^2}{2c^2}} \quad (2)$$

85
86 Where $w(m)$ is the window function (which is Gaussian in this study). In the Gaussian window a
87 is the height of the curve's peak, b is the position of the center of the peak and c is the standard
88 deviation. m and ω are discrete time shift and angular frequency respectively and $x[n]$ is the
89 seismic signal.

90

91 2.2. Mixed Components of STFT (MC-STFT)

92 The STFT of $x[n]$ can be interpreted as the Fourier transform of the product $x[n]w[n - m]$. So as
93 it is clear, in this study there is no changes in STFT formulation. The next step is to extract three
94 frequency component section from time-frequency domain obtained by applying STFT on each
95 seismic trace.

96

$$\begin{cases} \text{the first (f) component} = C_1(m, f_1), & f_1 = F_N/10 \\ \text{the second (f) component} = C_2(m, f_2), & f_2 = F_N/5 \\ \text{the third (f) component} = C_3(m, f_3), & f_3 = F_N/3 \end{cases} \quad (3)$$

97

98 Where F_N is the Nyquist frequency of seismic signals. Now these frequency components are
99 normalized so that the effect of intensity of each frequency will be the same. So they are denoted
100 by $C_{1,N}$, $C_{2,N}$ and $C_{3,N}$. And the final step is to multiply these component sections as below and
101 get the final image.

102

$$G(m, d_i) = (C_{1,N} * C_{2,N} * C_{3,N})_i \quad (4)$$

103

104 Where $G(m, d_i)$ is the final gas reservoir image and d_i is the horizontal distance in seismic zero-
105 offset section (i.e. the i th trace). To obtain a more accurate gas reservoir location we can do the
106 second iteration of this procedure. The first and the second iteration is summarized as below:

107

The algorithm of the first and second iteration of the method

$k = 1$, first iteration

1- $x_i[n]$, as the i th trace of zero – offset section

2- $X_{STFT, i, k}[m, f] = STFT(x_i[n])$

3- extracting $C_{1, N, k}$, $C_{2, N, k}$ and $C_{3, N, k}$

4- $G_{k, i}(m) = (C_{1, N, k} * C_{2, N, k} * C_{3, N, k})_i$

$k = 2$, second iteration

5- $G_{k-1, i}(m)$, as the i th signal of gas image section

6- $X_{STFT, i, k}[p, f] = STFT(G_{k-1, i}(m))$

7- extracting $C_{1, N, k}$, $C_{2, N, k}$ and $C_{3, N, k}$

8- $G_{k, i}(p) = (C_{1, N, k} * C_{2, N, k} * C_{3, N, k})_i$

108

109

110

111 2.3. Synchrosqueezing STFT (SSTFT)

112 The SSTFT is a combination of the STFT and the synchrosqueezing method. The
113 synchrosqueezing method use to sharpen the STFT map, and therefore, generates a concentrated
114 time–frequency map named SSTFT (Auger, 2013).

115 The SSTFT is given by

$$116 \quad SW_x(\tilde{\omega}_l, \tau) = (\Delta\tilde{\omega})^{-1} \sum_{\omega_k: |\tilde{\omega}(\omega_k, \tau) - \tilde{\omega}_l| \leq \Delta\tilde{\omega}/2} W_x(\omega_k, \tau) e^{i\omega_k \tau (\Delta\omega)_k} \quad (5)$$

118 Where

$$119 \quad \omega_k - \omega_{k-1} = (\Delta\omega)_k$$

120 This is the forward transform. The energies of the STFT be squeezed to the instantaneous
121 frequencies locations according to the equation (5) in order to get a concentrated time–frequency
122 representation.

123

124 **3. Results and Discussion**

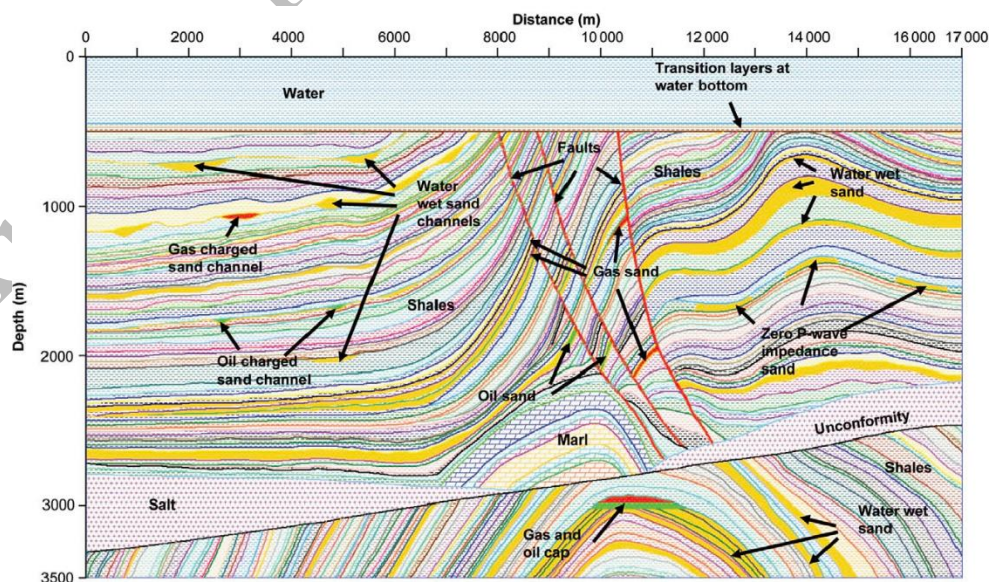
125 In this study we assess the performance of the proposed algorithms (i.e. both first and second
 126 iteration). We do this by three models, first with a real well-known Marmousi model then two
 127 other real models.

128

129 **3.1. Marmousi Model**

130 This model is a 3500 m of depth and 17000 m of distance in which there are some gas reservoirs
 131 (figure 1). We picked one of these reservoirs to test out algorithm. As it's shown in figure 1, there
 132 is a gas reservoir on top left of this geological section (Martin, 2006). So we cropped the original
 133 section, which is the pre-stack depth migration image of the area (figure 2), from 1875 m to 6250
 134 m in distance and from 0 s to 1.37 s in time (figure 2). The cropped section (figure 3) is then used
 135 to apply our algorithm on. The result of applying the first iteration of MC-STFT on this section
 136 leads to locating gas reservoir but there is still an anomaly at water bottom (figure 4a). Other
 137 anomalies but gas reservoir will be attenuated by second iteration (figure 4b). As it is clear from
 138 figure 4b, second iteration eliminates the water bottom effect and just gas reservoir anomaly can
 139 be seen. The result of SSTFT in figure 4c shows good performance of it, however the MC-STFT
 140 confirms the its power to localize gas reservoir zone.

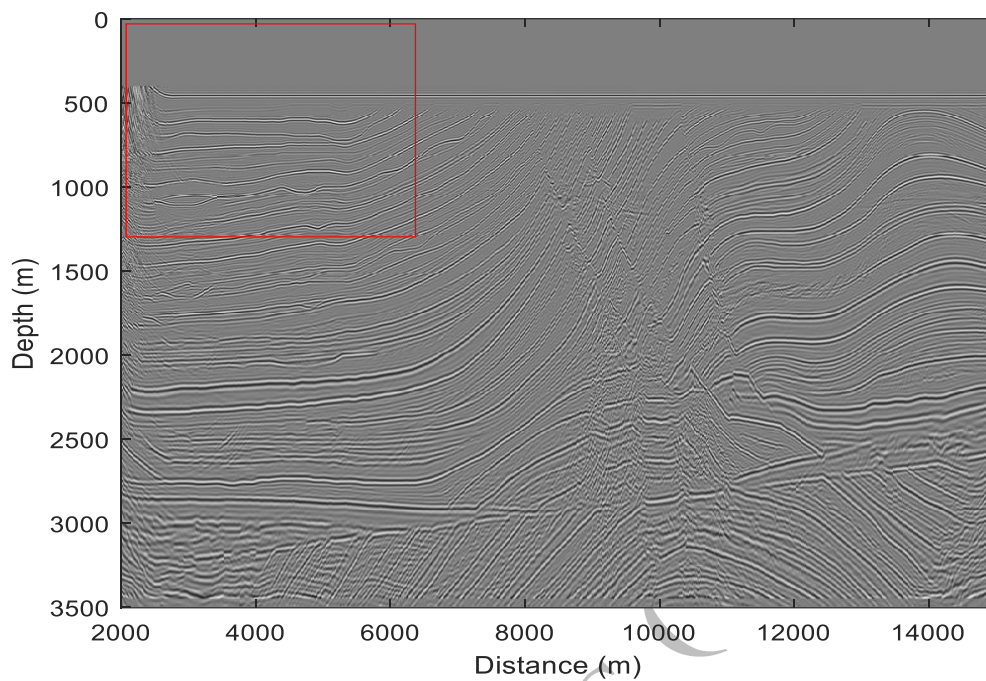
141



142

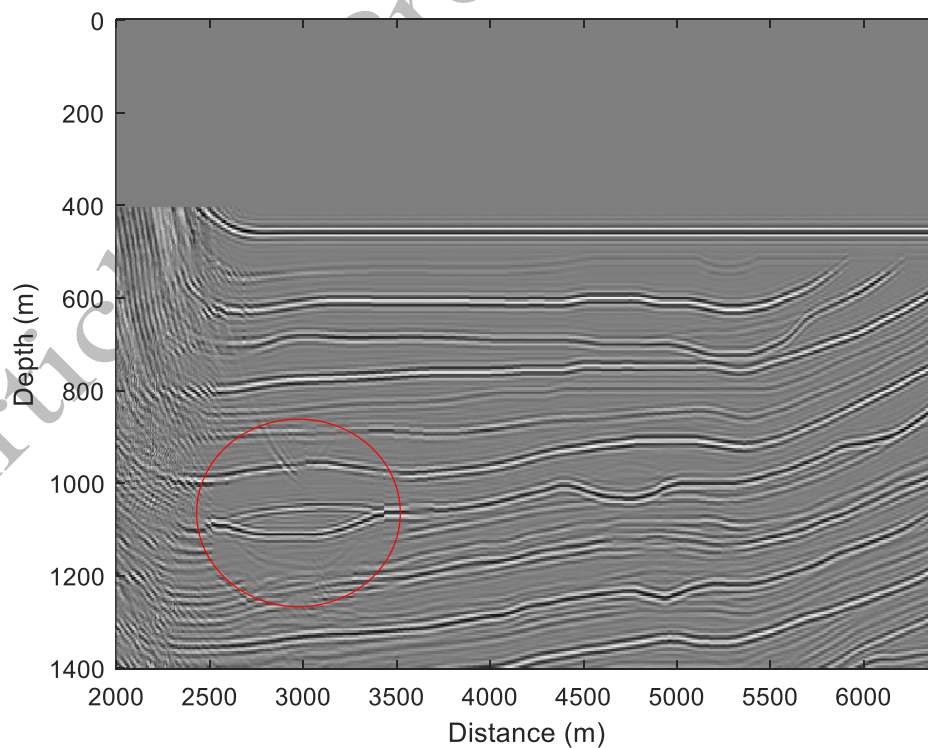
143
144

Figure 1. Marmousi model, structural elements, horizons and lithologies.



145
146
147

Figure 2. Marmousi zero-offset section (the red box shows the cropped part).

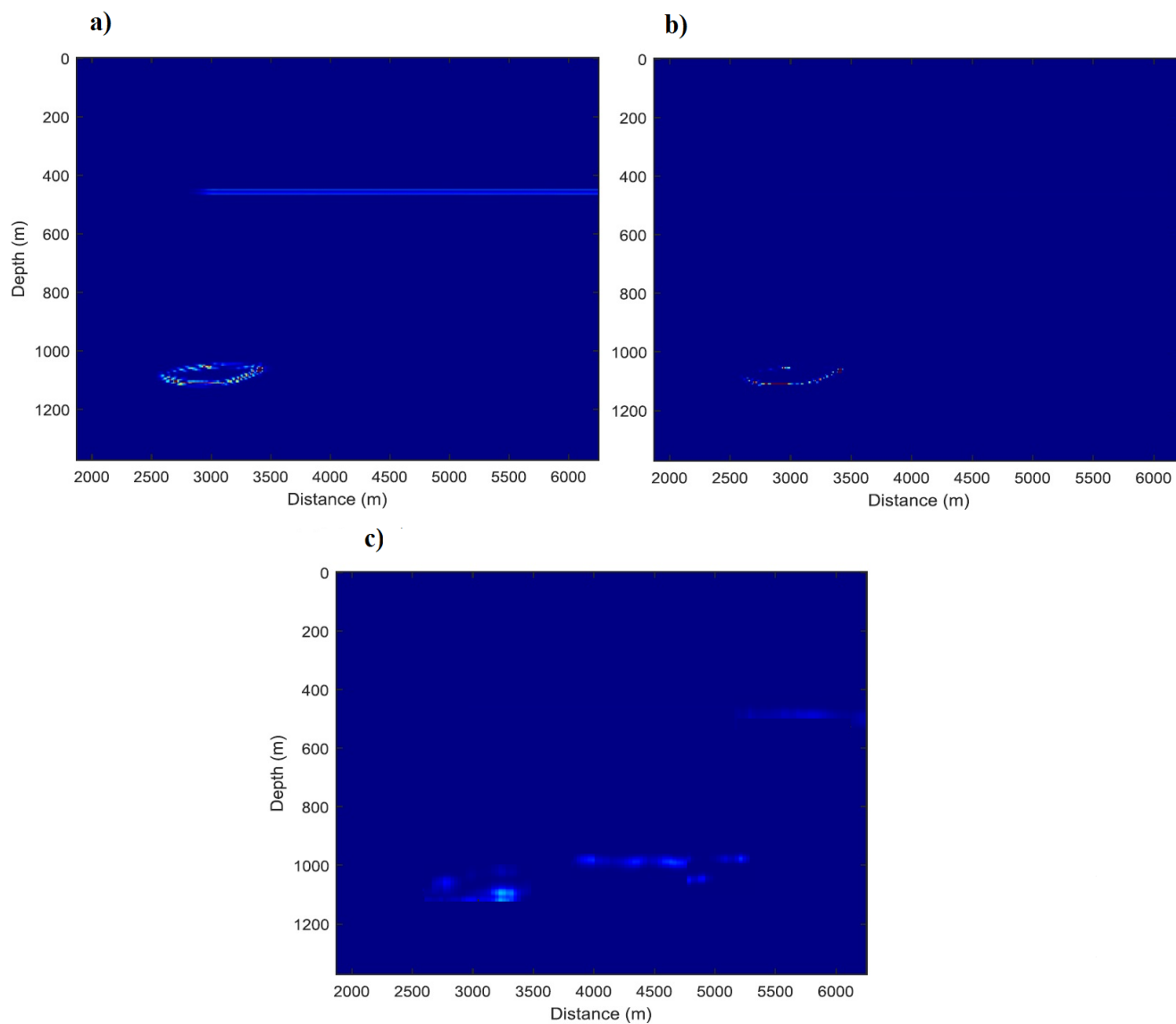


148
149

Figure 3. Marmousi cropped zero-offset section (the red circle represents the gas reservoir).

150

151



152

153 **Figure 4.** a) The first iteration of MC-STFT. Anomaly shows gas reservoir. b) The second iteration of
 154 MC-STFT. c) The result of SSTFT.

155

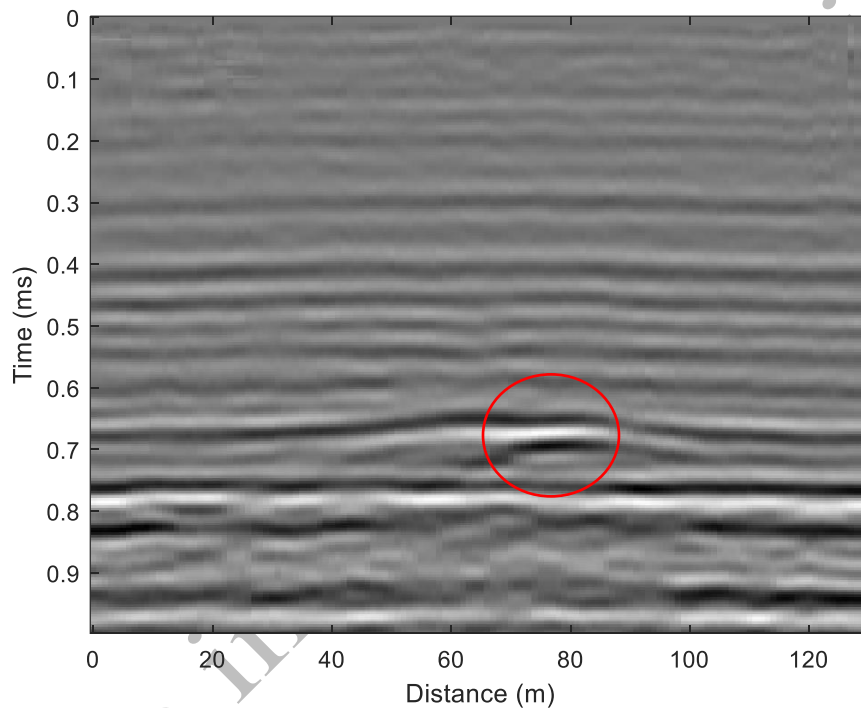
156 3.2. Real model 1

157 This model is a zero-offset section with 996 ms of time axis and 1310 m of distance (figure 5).

158 There is a gas reservoir in this model which is shown by the red circle. The first and second

159 iteration of the proposed algorithm are applied on this section. The first iteration bolds the gas

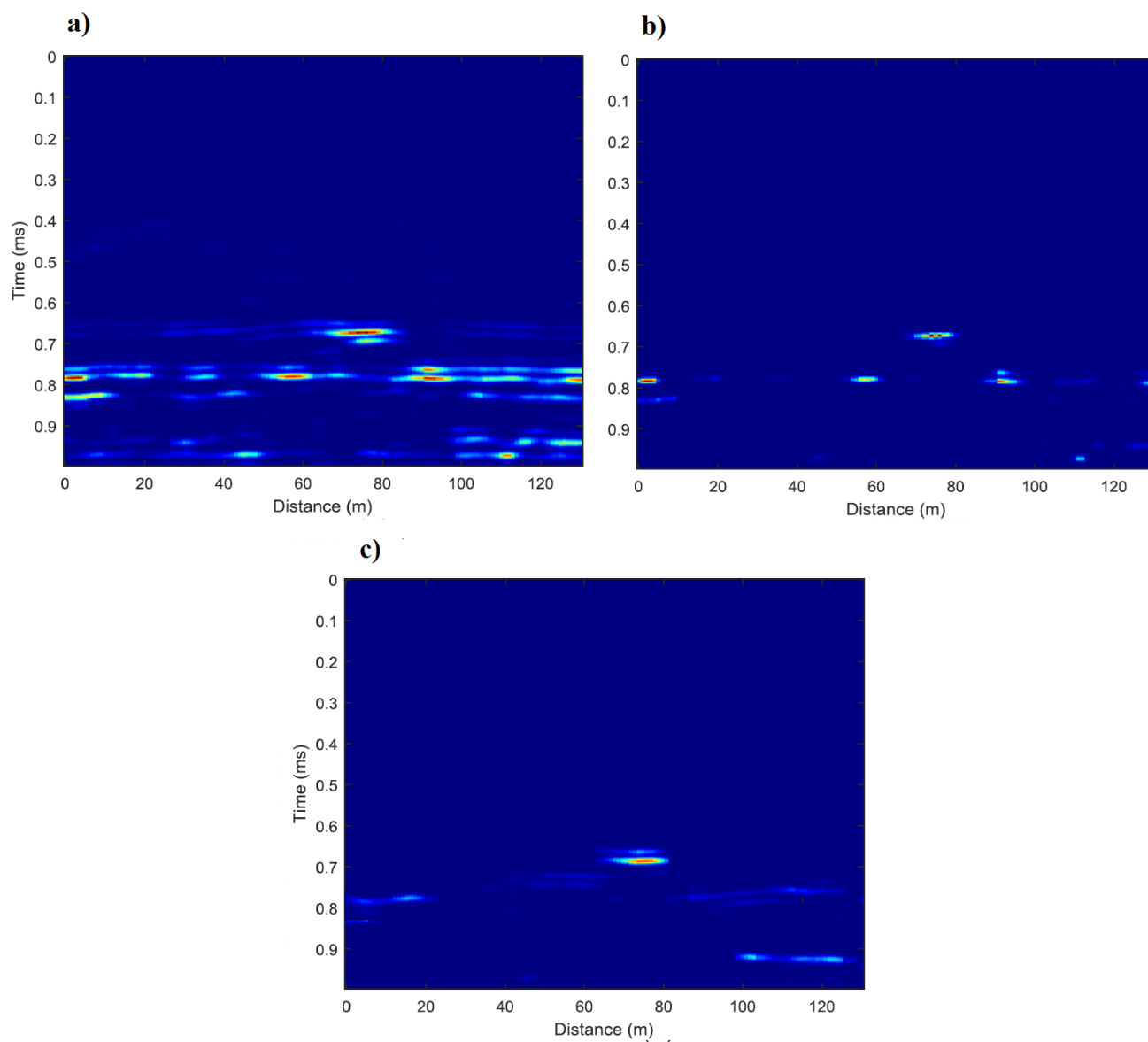
160 reservoir in such a way that there is an anomaly in gas area (figure 6a). Although there are still
161 some slight anomalies on other parts of the section, for example on the bottom of the section
162 another of anomalies can be seen. However, the peak of the amplitudes lies on the gas area. The
163 second iteration, on the other hand, located the gas reservoir more accurately and increased the
164 detection resolution (figure 6b). Figure 6c shows the output of SSTFT, the good performance of
165 it is clear but not same as second iteration of MC-STFT.
166



167

168

Figure 5. zero-offset section in which the gas reservoir is represented by the red circle.



169

170 **Figure 6.** a) Gas reservoir anomaly after the first iteration of MC-STFT. b) The section after the second
 171 iteration of MC-STFT. c) The result of SSTFT.

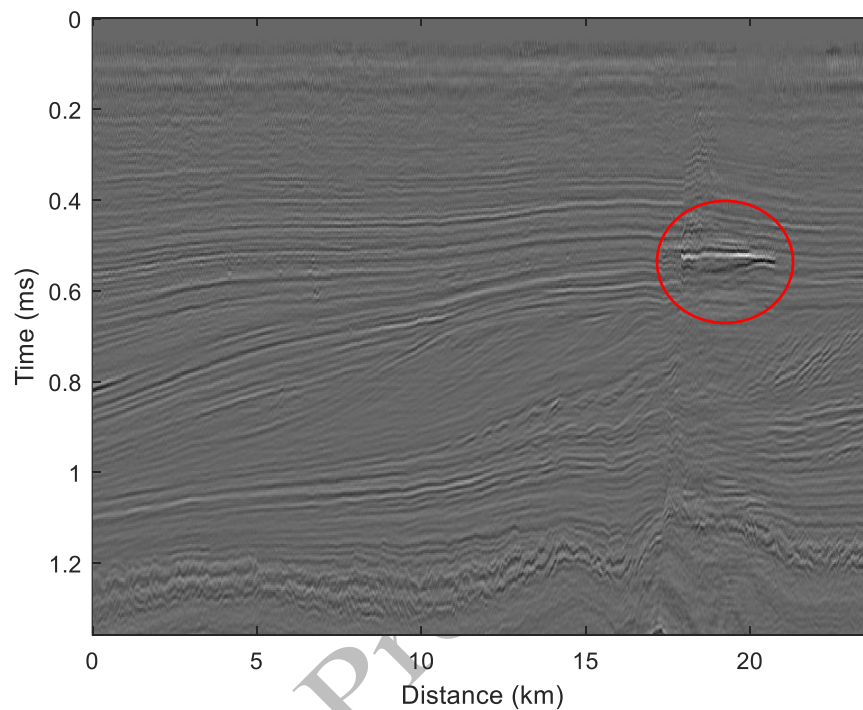
172

173 3.3. Real model 2

174 This model is a block in the Dutch sector of the North Sea which is a zero-offset section with 1356
 175 ms of time axis and 23.75 km of distance (figure 7). The gas reservoir is located approximately on
 176 the middle right part of the section which is shown by the red circle. [The first and second iteration](#)
 177 [of MC-STFT are applied on this section. The first iteration is able to distinguish gas reservoir](#)

178 accurately enough (figure 8a). The remaining anomalies which might be misleading in locating
179 gas reservoir will be considerably vanished by the second iteration of MC_STFT (figure 8b).
180 Applying result of SSTFT is shown in figure 8c and it succeeded to identify the gas zone with high
181 resolution.

182

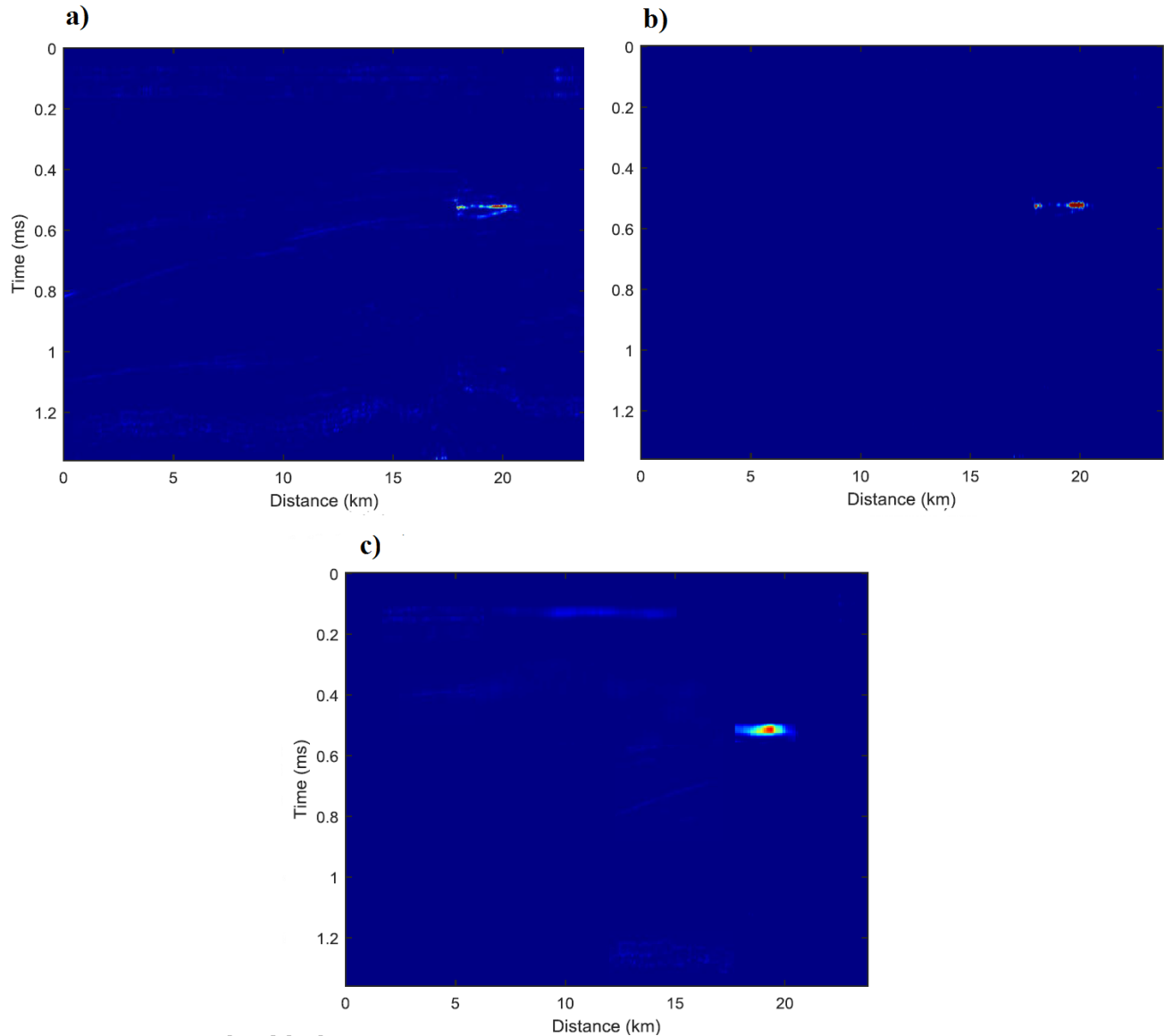


183

184 **Figure 7.** North Sea zero-offset section and the gas target.

185

186



187

188 **Figure 8.** a) The result of applying first iteration of MC-STFT. b) Second iteration output of MC-STFT. c)

189 The result of SSTFT.

190

191

192 STFT offers a compromise between time and frequency resolution, which is controlled by the

193 window size used during the transformation process. Although STFT provides a constant time

194 frequency resolution across all frequencies, this can limit its effectiveness in analyzing signals with

195 rapid transient changes because it cannot adapt its resolution to signal characteristics dynamically.

196 This investigation has demonstrated that while STFT offers a straightforward and computationally

197 efficient approach, it is constrained by a fixed time-frequency resolution trade-off, which may not
198 adequately capture the intricate dynamics of signals with rapidly varying frequencies.

199

200 **4. Conclusion**

201 In this study we employed STFT in an algorithm to detect gas reservoirs from seismic zero-offset
202 sections. This method adds no complexity to STFT methodology and uses the simple original
203 STFT. In fact, extracting three components of STFT of the zero-offset section and multiply them
204 is the key that creates this attribute. Two iterations of this algorithm is proposed so that the first
205 one distinguishes the gas reservoir with high accuracy from other events. Consequently, the second
206 iteration increases detection resolution and makes an absolutely precise image. MC-STFT for all
207 of its potential, seismic data are subject to a wide variety of noise related problems that can and do
208 limit its usefulness, Therefore, in the first stage, pre-processing is needed. In addition, the fixed
209 window size used in STFT can be a significant limitation, as it imposes a trade-off between time
210 and frequency resolution. Narrow windows give good time but poor frequency resolution, and vice
211 versa. However, simplicity and efficiency can make a method superior. Results, which tested the
212 proposed algorithm on three real data, also show that the first iteration of MC-STFT is able to
213 locate gas reservoirs but with some other weak amplitude anomalies. But taking advantage of the
214 second iteration of this method considerably increases the accuracy of gas reservoir location. Also
215 it should be mentioned, the steps and parameters of the designed algorithm could be optimized in
216 future work to improve its performance for gas reservoir identification. To evaluate the proposed
217 method, SSTFT is also employed and applied to the data, the outputs show its power to localize
218 and identify gas zone. Totally, the final results approved more power and higher resolution of MC-
219 STFT in comparison with SSTFT for gas reservoir detection.

220

221 **Declaration of interests**

222 The authors declare that they have no known competing financial interests or personal
223 relationships that could have appeared to influence the work reported in this paper.

224

225

226

227 **References**

- 228 Auger F, Flandrin P and Lin Y T (2013) Time-frequency reassignment and synchrosqueezing: an
229 overview *IEEE Signal Process.* 30 32–41.
- 230 Barabadi, Mahdi, Mohammad Radad, and Amin Roshandel Kahoo. (2024) "Seismic data AVO
231 analysis in time frequency domain using synchroextracting transform." *Journal of Applied*
232 *Geophysics* 224, 105364.
- 233 Castagna, J. P., Shengjie, S., & Robert W. (2003) Siegfried. "Instantaneous spectral analysis:
234 Detection of low-frequency shadows associated with hydrocarbons." *The leading edge* 22, no.
235 2: 120-127.
- 236 Chen, Y., Tingting, L., Xiaohong, C., Jingye, L., & Erying, W. (2014) "Time-frequency analysis
237 of seismic data using synchrosqueezing wavelet transform." *2014 SEG Annual Meeting*.
238 OnePetr.
- 239 Cohen, L., (1989) "Time-frequency distributions-a review." *Proceedings of the IEEE* 77, no. 7
240 (1989): 941-981.
- 241 Gao, J., Xiaolong D., Wen-Bing W., Youming L., & Cunhuan P. (1999) "Instantaneous parameters
242 extraction via wavelet transform." *IEEE transactions on geoscience and remote sensing* 37, no.
243 2: 867-870.
- 244 Li, Y., & Xiaodong, Z. (2008) "Spectral decomposition using Wigner-Ville distribution with
245 applications to carbonate reservoir characterization." *The Leading Edge* 27, no. 8: 1050-1057.
- 246 Liu, G., Sergey, F., & Xiaohong C. (2011) "Time-frequency analysis of seismic data using local
247 attributes." *Geophysics* 76, no. 6: P23-P34.
- 248 Lu, W., & Qiang, Z. (2009) "Deconvolutive short-time Fourier transform spectrogram." *IEEE*
249 *Signal Processing Letters* 16, no. 7: 576-579.
- 250 Lu, W., & Fangyu, L. (2013) "Seismic spectral decomposition using deconvolutive short-time
251 Fourier transform spectrogram." *Geophysics* 78, no. 2: V43-V51.
- 252 Martin, G. S., Robert, W., & Kurt, J. M. (2006) "Marmousi2: An elastic upgrade for
253 Marmousi." *The leading edge* 25, no. 2: 156-166.
- 254 Mateo, Carlos, and Juan Antonio Talavera. "Bridging the gap between the short-time Fourier
255 transform (STFT), wavelets, the constant-Q transform and multi-resolution STFT." *Signal,*
256 *Image and Video Processing* 14.8 (2020): 1535-1543.
- 257 Odegard, J. E., Richard, G. B., & Kurt L. O. (1997) "Instantaneous frequency estimation using the
258 reassignment method." In *SEG Technical Program Expanded Abstracts 1997*, pp. 1941-1944.
259 Society of Exploration Geophysicists.

- 260 Partyka, G., James, G., & John L. (1999) "Interpretational applications of spectral decomposition
261 in reservoir characterization." *The leading edge* 18, no. 3: 353-360.
- 262 Quan, Y., & Jerry M. H. (1997) "Seismic attenuation tomography using the frequency shift
263 method." *Geophysics* 62, no. 3: 895-905.
- 264 Reine, C., Mirko V., & Roger, C. (2009) "The robustness of seismic attenuation measurements
265 using fixed-and variable-window time-frequency transforms." *Geophysics* 74, no. 2: WA123-
266 WA135.
- 267 Shirazi, Mahmoud, et al. (2023) "Detecting Shallow Gas Reservoir in the F3 Block, the
268 Netherlands, Using Offshore Seismic Data and High-Resolution Multi-Synchrosqueezing
269 Transform." *Natural Resources Research*, 32.5, 2007-2035.
- 270 Siddique, Muhammad Farooq, et al. "A Hybrid Deep Learning Approach: Integrating Short-Time
271 Fourier Transform and Continuous Wavelet Transform for Improved Pipeline Leak Detection."
272 *Sensors* 23.19 (2023): 8079.
- 273 Sinha, S., Partha S. R., Phil, D. A. & John, P. C. (2005) "Spectral decomposition of seismic data
274 with continuous-wavelet transform." *Geophysics* 70, no. 6: P19-P25.
- 275 Wu, G., & Yatong, Z. (2018) "Seismic data analysis using synchrosqueezing short time Fourier
276 transform." *Journal of Geophysics and Engineering* 15, no. 4: 1663-1672.
- 277 Yang, Yang, et al. "Parameterised time-frequency analysis methods and their engineering
278 applications: A review of recent advances." *Mechanical Systems and Signal Processing* 119
279 (2019): 182-221.
- 280 Zhang, Dengsheng, and Dengsheng Zhang. "Wavelet transform." *Fundamentals of image data
281 mining: Analysis, Features, Classification and Retrieval* (2019): 35-44.
- 282 Zhou, J., Jing, B., John, P., Castagna, Q., Guo, C. Yu., & Ren, J. (2019) "Application of an STFT-
283 based seismic even and odd decomposition method for thin-layer property estimation." *IEEE
284 Geoscience and Remote Sensing Letters* 16, no. 9: 1348-1352.
- 285 Zhuang, Cuifang, and Ping Liao. "An improved empirical wavelet transform for noisy and non-
286 stationary signal processing." *IEEE Access* 8 (2020): 24484-24494.